Original papers
Manufacturing processes and systems

УДК 66.02:66.097.3:66.097.5 DOI: 10.17277/jamt-2025-10-04-290-300

Synthesis of Co-Mn/diatomite composites by low-temperature combustion

© Roza I. Jussupkaliyeva[a]✉, Vyacheslav N. Borshch[b], Inna M. Bystrova[b], Elena V. Pugacheva[b], Natalia Yu. Khomenko[b], ArtemV. Rukhov[c], Svetlana I. Pomogailo[b,d]

[a] *Zhangir Khan West Kazakhstan Agrarian Technical University, 51, Zhangir Khan St., Uralsk, 090009, Republic of Kazakhstan,*
[b] *Merzhanov Institute of Structural Macrokinetics and Materials Science, Russian Academy of Science, 8, Academician Osipyan St., Chernogolovka, 142432, Russian Federation,*
[c] *Tambov State Technical University, Bld. 2, 106/5, Sovetskaya St., Tambov, 392000, Russian Federation,*
[d] *All-Russian Institute for Scientific and Technical Information, 20, Usievich St., Moscow, 125190, Russian Federation*

✉ rozaid2@mail.ru

Abstract: Co-Mn-containing composites based on diatomite as a carrier (matrix) were prepared using the energy-efficient low-temperature combustion method using natural and activated diatomite from the Utesai deposit (Republic of Kazakhstan) as a support (matrix). Activation included the stages of washing with water, calcination at 500 °C, and treatment with an HCl solution in various combinations. The phase containing 5 wt. % of Co + 5 wt. % of Mn (calculated as metals) was applied to diatomite by low-temperature combustion of a mixture of Co and Mn nitrates (oxidizers) with urea (reducing agent, fuel) applied to diatomite. The maximum temperature in the combustion wave reached 337 °C. The physicochemical properties of the composites were studied using X-ray diffraction, SEM/EDS, and the specific surface area was measured according to BET on nitrogen. The main phases in the composites, according to XRD data, were modifications of SiO_2 (quartz, tridymite, and cristobalite). According to the SEM/EDS results, there is an uneven distribution of the Co-Mn-containing phase components over the surface of the catalyst granules, due to the heterogeneity of the surface morphology and internal pores of natural diatomite. Impurity elements (Mg, Al, Na, K, Ca, Fe) were also detected in the composition of the supports and catalysts. The specific surface area of the support samples ranged from 56.0 to 83.5 $m^2 \cdot g^{-1}$, and that of the composites – from 46.4 to 78.5 $m^2 \cdot g^{-1}$. The resulting composites are expectedto be used as catalysts for deep oxidation of CO and hydrocarbons for environmentally important technologies for the neutralization of man-made exhaust and waste gases.

Keywords: diatomite; activation; low-temperature combustion; cobalt; manganese; composites.

For citation: Jussupkaliyeva RI, Borshch VN, Bystrova IM, Pugacheva EV, Khomenko NYu, Rukhov AV, Pomogailo SI. Synthesis of Co-Mn/diatomite composites by low-temperature combustion. *Journal of Advanced Materials and Technologies*. 2025;10(4):290-300. DOI: 10.17277/jamt-2025-10-04-290-300

Синтез композитов состава Co-Mn/диатомит методом низкотемпературного горения

© Р. И. Джусупкалиева[a]✉, В. Н. Борщ[b], И. М. Быстрова[b], Е. В. Пугачева[b], Н. Ю. Хоменко[b], А. В. Рухов[c], С. И. Помогайло[b,d]

[a] *Западно-Казахстанский аграрно-технический университет им. Жангир хана, ул. Жангир хана, 51, Уральск, 090009, Республика Казахстан,*
[b] *Институт структурной макрокинетики и проблем материаловедения им. А. Г. Мержанова РАН, ул. Академика Осипьяна, 8, Черноголовка, 142432, Российская Федерация,*
[c] *Тамбовский государственный технический университет, ул. Советская, 106/5, пом. 2, Тамбов, 392000, Российская Федерация,*
[d] *Всероссийский институт научной и технической информации РАН, ул. Усиевича, 20, Москва, 125190, Российская Федерация*

✉ rozaid2@mail.ru

Аннотация: Энергоэффективным методом низкотемпературного горения получены Co-Mn-содержащие композиты на основе природного и активированного диатомита Утесайского месторождения (Республика Казахстан) в качестве носителя (матрицы). Активация включала этапы промывки водой, прокалки при 500 °C,

а также обработки раствором HCl, в различных сочетаниях. Нанесение фазы, содержащей 5 мас. % Co + 5 мас. % Mn (в расчете на металлы), на диатомит производили путем низкотемпературного горения смеси нитратов Co и Mn (окислители) с мочевиной (восстановитель, горючее). Максимальная температура в волне горения достигала 337 °C. Исследованы физико-химические свойства композитов методами РФА, СЭМ/ЭДС, и измерена удельная поверхность по адсорбции азота. Основными фазами в составе композитов по данным РФА являлись модификации SiO_2 (кварц, тридимит и кристобалит). Согласно результатам СЭМ/ЭДС, имеет место неравномерное распределение компонентов Co-Mn-содержащей фазы по поверхности гранул катализаторов, связанное с неоднородностью морфологии поверхности и внутренних пор природного диатомита. Также были обнаружены примесные элементы (Mg, Al, Na, K, Ca, Fe). Удельная поверхность по БЭТ образцов носителей составила от 56,0 до 83,5 $м^2$/г, а композитов – от 46,4 до 78,5 $м^2$/г. Полученные композиты предполагается использовать как катализаторы процесса глубокого окисления CO и углеводородов для экологически важных технологий нейтрализации выхлопных и отходящих газов техногенной природы.

Ключевые слова: диатомит; активация; низкотемпературное горение; кобальт; марганец; композиты.

Для цитирования: Jussupkaliyeva RI, Borshch VN, Bystrova IM, Pugacheva EV, Khomenko NYu, Rukhov AV, Pomogailo SI. Synthesis of Co-Mn/diatomite composites by low-temperature combustion. *Journal of Advanced Materials and Technologies*. 2025;10(4):290-300. DOI: 10.17277/jamt-2025-10-04-290-300

1. Introduction

Diatomite is a sedimentary rock formed from the remains of diatomaceous algae, with abundant deposits in Kazakhstan and Russia [1, 2]. The main component of diatomite is silica SiO_2 (70–98 wt. %, depending on the deposit), largely in an amorphous state. Its characteristic feature is a highly porous structure, resulting in a low density (on average 0.5–0.7 $g \cdot cm^{-3}$), a high specific surface area, high adsorption capacity, and low thermal conductivity. Furthermore, it is quite heat-resistant and resistant to aggressive environments. Due to these properties, as well as its low cost, diatomite is widely used in various industries and construction. Thus, in its original or modified forms, it is an effective sorbent for removing oil spills and waste containing petroleum products [3], water purification from aromatic compounds and esters [4], inorganic salts, in particular, phosphates (in combination with $Mg(OH)_2$ [5]). Particular attention is paid to the development of diatomite-based adsorbents for the removal of organic dyes from waste and discharge water [6, 7]. High specific surface area and chemical stability are attractive factors for the use of diatomite as a carrier of deposited catalysts for various processes. The range of developed diatomite-based catalysts is currently quite wide. Diatomite modified with organoaluminum compounds turned out to be an active catalyst for ethylene polymerization [8]; with deposited transition metal salts it showed high activity in the process of catalytic pyrolysis of the propane-butane fraction to obtain multiwalled carbon nanotubes [9]. Diatomite-based catalysts have demonstrated high selectivity in the isomerization of α-pinene [10], the hydrogenation of vegetable oils to particularly valuable cis-isomers [11], and the hydrogenation of CO_2 to methane [12]. Developments have been made of catalysts for the deep oxidation of CO and propane [13], formaldehyde [14, 15], and the liquid-phase oxidation of As(III) compounds in an alkaline medium [16]. Catalysts for photooxidation processes in both gaseous and liquid media, including those for water purification processes, are being intensively developed [17–21].

The most common method for synthesizing supported catalysts is the impregnation of carriers with solutions of active transition metal salts (most often nitrates), followed by drying and calcination [9, 23]. The disadvantage of this method is the high calcination temperature (usually not less than 500 °C) and the corresponding energy costs, as well as toxic gas emissions containing nitrogen oxides. An alternative to this method is the relatively recently developed energy-efficient method of self-propagating surface thermal synthesis or the low-temperature combustion method [24–32]. Its essence lies in impregnating the carrier with a mixture of solutions of an oxidizer (usually transition metal nitrates) and a reducing agent (fuel) – a water-soluble organic compound (urea, glycine, citric acid, sucrose, sorbitol, etc.). After drying, slight heating (< 200 °C) initiates a self-sustaining combustion reaction in the sample, usually proceeding in a wave mode. The gaseous products of combustion are water vapor, CO_2, and, in the case of nitrogen-containing fuels, N_2. The resulting catalysts often have a nanosized active phase, which contributes to their high activity and selectivity. We previously used this method to obtain a number of catalysts for the deep oxidation of CO and propane, as well as the hydrogenation of CO_2 [29–32, 36] on a wide range of supports (γ-Al_2O_3,

silica gel (including modified Al_2O_3), zeolites NaX and ZSM-5, halloysite (natural aluminosilicate nanotubes), and the natural silica mineral opoka). The catalysts demonstrated high activity, selectivity, and stability in the processes studied. In [29], we were the first to show that this method can be used to obtain not only oxide but also metallic phases of transition metals in the catalyst composition.

In this study, a low-temperature combustion method was used to obtain composites containing Co-Mn phases based on the initial and activated diatomite. These composites are expected to be used in the future as catalysts for the deep oxidation of CO and hydrocarbons for environmentally important technologies for the neutralization of exhaust and waste gases of anthropogenic origin. The composition of the Co-Mn-containing phase was selected based on the results of our previous studies and literature data [23, 29, 33–36], which showed that catalysts supported on various supports with a bimetallic active phase Co-Mn were characterized by high activity and stability in the process of deep oxidation of CO and propane. The study was aimed at studying the features of the synthesis process of various samples of the Co-Mn/diatomite system, and the physicochemical characteristics of the obtained materials.

2. Materials and Methods

2.1. Composite preparation

2.1.1. Preparation of the carrier

Diatomite from the Utesai deposit in the Republic of Kazakhstan was used as the carrier for the composites. All carrier samples were crushed to a 0.1–0.3 mm fraction using sieves, pre-washed several times with distilled water to remove water-soluble impurities and easily dispersible clay impurities, and dried in an oven at 90 °C. Samples that did not undergo further processing are designated D1. The next subset of samples were calcined at 500 °C for 3 hours, washed again with distilled water, and dried in an oven at 90 °C (D2). The third part of the carriers was washed with a 10 % HCl solution to remove impurities of carbonates, oxides and hydroxides of alkaline earth metals and iron, then washed with distilled water until a neutral reaction and dried in a drying oven at 90 °C (D3). The fourth part of the samples was washed with a 10 % HCl solution, then washed with distilled water until a neutral reaction, dried in a drying oven at 90 °C, calcined at 500 °C for 3 hours and again washed with distilled water and dried at 90 °C (D4).

2.1.2. Synthesis of composites by low-temperature combustion

The support samples prepared in accordance with section 2.1.1 were impregnated with a mixture of cobalt nitrate hydrate solutions $Co(NO_3)_2{\cdot}6H_2O$ and manganese $Mn(NO_3)_2{\cdot}4H_2O$ (oxidizers), and urea $CO(NH_2)_2$ (reducing agent, fuel). The required amount of precursors to obtain a composite containing 5 wt. % of Co and 5 % wt. % of Mn (calculated as metals) was calculated using the following equation:

$$Co(NO_3)_2{\cdot}6H_2O + Mn(NO_3)_2{\cdot}4H_2O + 4CO(NH_2)_2 \rightarrow$$
$$\rightarrow Co + Mn + 4CO_2 + 5N_2 + 18H_2O. \quad (1)$$

Thus, the maximum amount of reducing agent (urea) was introduced into the precursor mixture, sufficient to obtain the fully reduced (metallic) phases of Co and Mn. This limiting case is far from always realized; a mixture of metallic and oxide phases [29], or even oxide phases alone, was often obtained. In any case, unreacted fuel was simply washed from the sample. The proposed metal content is the minimum possible for achieving stable low-temperature combustion.

The calculated amounts of nitrates and urea were dissolved in a minimal amount of water at room temperature, and the carrier samples were impregnated with the resulting solution while stirring. After drying in a drying oven at 90 °C, 10 g of the samples were placed in a combustion reactor assembled according to the diagram in Fig. 1.

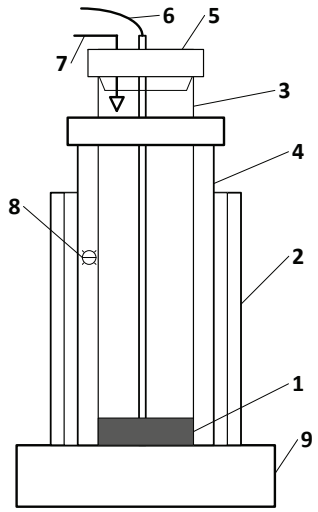

Fig. 1. A diagram of the experimental setup for synthesis in the low-temperature combustion mode: *1* – sample; *2* – heat-insulating casing with a viewing window; *3* – tubular quartz reactor with a flat bottom; *4* – quartz glass with a lid; *5* – dust collection system; *6* – thermocouple; *7* – argon supply; *8* – backlight lamp; *9* – electric heater

Throughout the experiment, the reactor was purged with argon. The reactor bottom heater was turned on and its power remained constant throughout the entire process. Temperature was monitored with a thermocouple placed in the sample layer at the center of the reactor bottom. Thermocouple readings were entered into a computer using a Metex ME-31 digital multimeter (Metex, Korea), and thermograms of the process were plotted as a temperature-time dependence. The sample combustion reaction began at a random point near the reactor perimeter and proceeded as a combustion wave, appearing as a darkening wave accompanied by intense gas evolution and dust emission above the sample layer. After cooling, the sample in the reactor under argon was stabilized with a 5 % H_2O_2 solution to prevent spontaneous combustion of any highly dispersed metallic phases in the active phase. The sample was then rinsed with distilled water and then dried at 90 °C. The fraction < 0.1 mm was removed from the resulting product by sifting on a sieve.

The prepared samples have the following designations: 5Co5Mn/D1, 5Co5Mn/D2, 5Co5Mn/D3, 5Co5Mn/D4. The numbers before the names of the elements indicate their content in the composites in wt. %, calculated as metal.

2.2. Physicochemical studies of samples

The X-ray diffraction (XRD) analysis of the samples was performed on a DRON-3M diffractometer (Russia), using FeKα radiation. Surface morphology and elemental composition were analyzed using a scanning electron microscope with an EDS attachment (SEM/EDS) (Zeiss Ultra plus microscope + INCA Energy 350 XT energy-dispersive spectrometer). Specific surface area was measured using a dedicated laboratory setup designed and constructed according to the design and methodology of Russian Standard 23401-90, using a multipoint scheme at liquid nitrogen temperature. Specific surface area was calculated using the BET method.

3. Results and Discussion

Figure 2 shows thermograms of the synthesis processes of composite samples on all types of supports. T_S denotes the point of temperature rise at the front of the combustion wave incident on the thermocouple, when the heat release from the chemical reaction begins to exceed the external heat input. In essence, this value is close to the autoignition temperature. The T_S values are quite close for all samples. Tmax correspond to the maximum temperatures in the combustion wave; the spread of their values is more significant (~50 °C). The splitting of the maximum temperature peaks (Fig. 2) was previously observed in the case of the synthesis of Co-Mn/γAl_2O_3 catalysts [29] and was explained as the passage of combustion and afterburning waves associated with the heterogeneity of the porous structure of the samples and the complex mechanism of the process, including the autocatalytic action of newly formed oxo-metallic phases.

The X-ray diffraction results for the support and composite samples are shown in Fig. 3. As can be seen, the diffraction patterns of both the support and the resulting composites show only peaks corresponding to three different SiO_2 modifications: quartz, cristobalite, and tridymite. Thus, support activation and composite synthesis do not significantly affect their phase structure. Co- and Mn-containing phases were not detected, apparently due to their content being below the detection limit of the method (~5 %) and the significant amorphous nature of the support.

In order to study the phase composition of the cobalt-manganese phase, the samples of 5Co5Mn/D1 and 5Co5Mn/D2 composites were boiled for 1 hour in a 20 % NaOH solution according to our previously proposed method [29], washed with distilled water until a neutral reaction was achieved, and dried at 90 °C. As a result, the amorphous component of the carriers dissolved, increasing the content of the Co-Mn component in the residue. The mass loss of the 5Co5Mn/D2 sample was 55.47 %, while that of the 5Co5Mn/D4 sample was 58.27 %. The X-ray diffraction results of the leached composite samples are shown in Fig. 4.

As can be seen, the next phase, $Co_xMn_yO_z$, is observed. This phase is a mixed oxide, meaning that reduction during combustion according to reaction (1) is incomplete.

The results of specific surface area measurements for the initial and activated support samples, as well as the Co-Mn-containing composites based on them, are shown in the histogram in Fig. 5.

As can be seen, the processing processes affect the specific surface area differently compared to the original diatomite sample. A slight decrease is observed only during the initial calcination of the diatomite, but the acid treatment and calcination processes lead to a significant increase in the specific surface area, reaching a maximum in the case of sample D4.

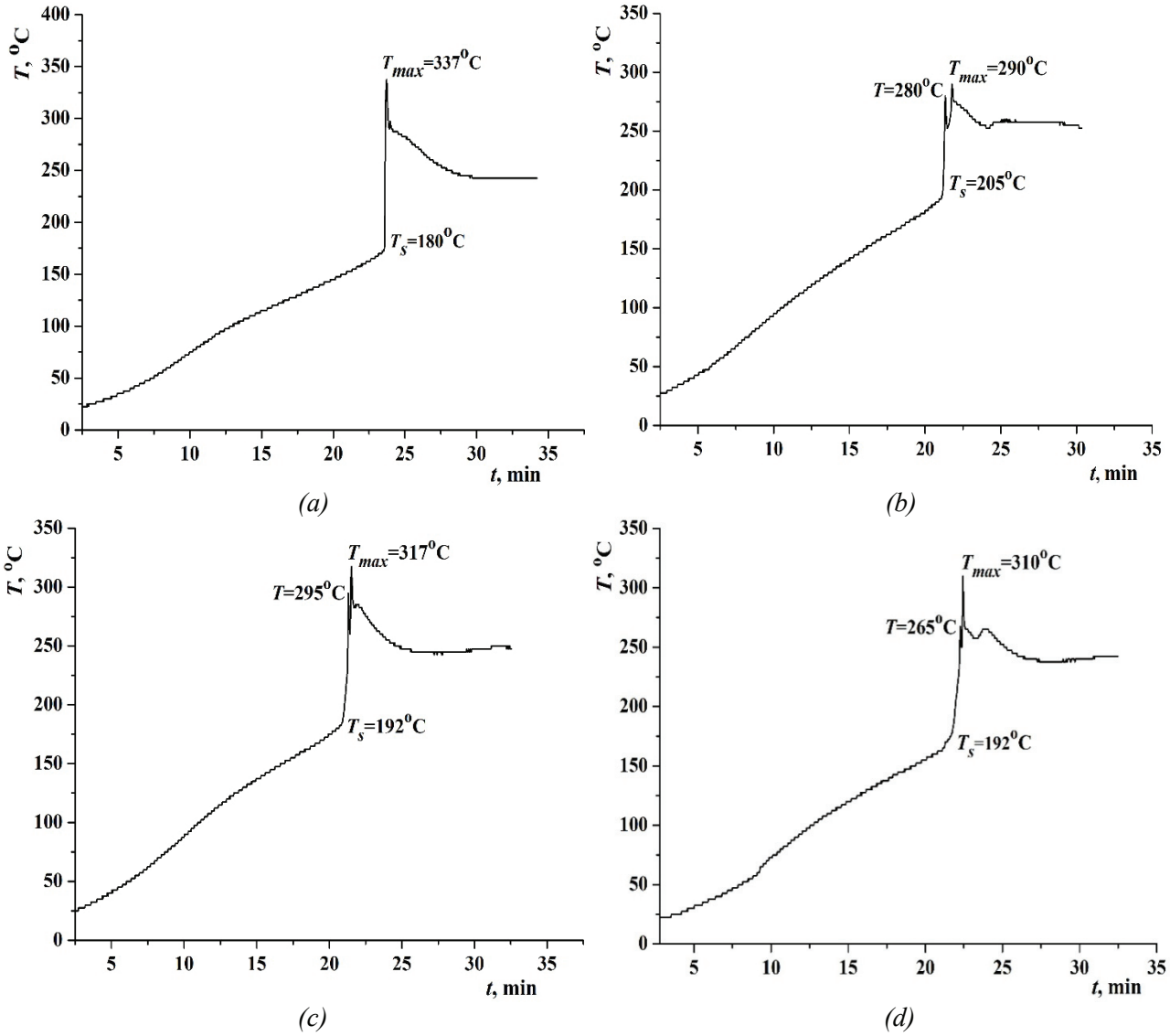

Fig. 2. Thermograms of the composite's synthesis process:
a – 5Co5Mn/D1; *b* – 5Co5Mn/D2; *c* – 5Co5Mn/D3; *d* – 5Co5Mn/D4

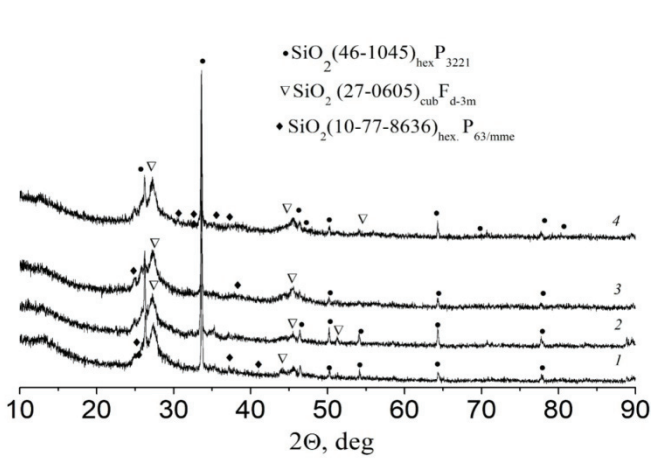

Fig. 3. XRD-patterns of samples:
1 – D1; *2* – D2; *3* – 5Co5Mn/D1; *4* – 5Co5Mn/D2

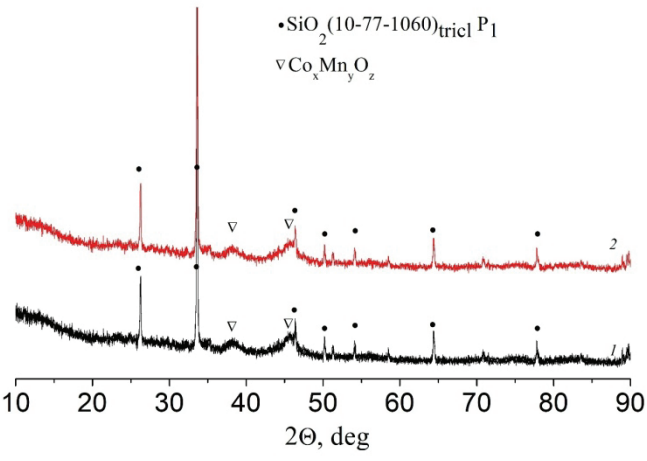

Fig. 4. XRD-patterns of leached composite samples:
1 – 5Co5Mn/D2; *2* – 5Co5Mn/D4

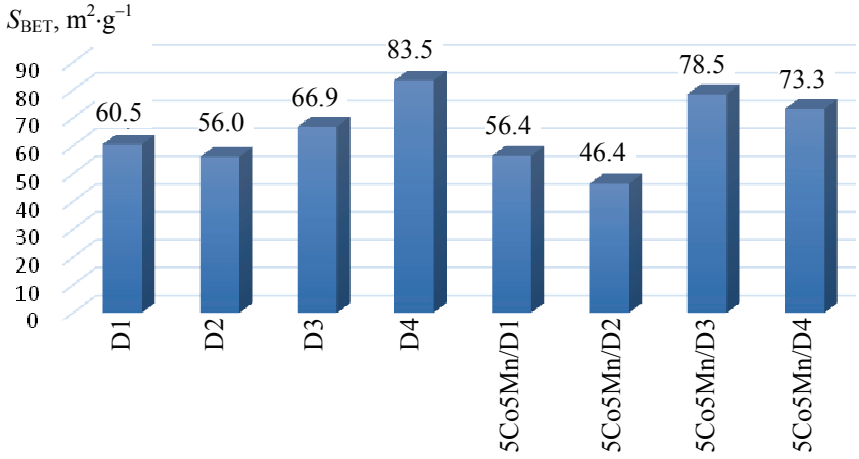

Fig. 5. Histogram of specific surface area values of support and composite samples

This is likely due to the opening of small pores in the support. The application of the Co-Mn-containing phase leads to a nearly identical dependence of the specific surface area of the composites on the specific surface area of the supports (except for the 5Co5Mn/D3 sample), with a slight decrease in the specific surface area of the composites. This suggests that the dispersion of the metal-containing phase is somewhat lower than the characteristic pore size of the support, as a result of which some of the small pores of the support may be blocked by particles of the applied phase. It should be noted that the specific surface area of the composites obtained in this study is significantly (by approximately 15 $m^2 \cdot g^{-1}$) higher than that of the 5Co5Mn/flask composites obtained by us previously [36], which demonstrated high catalytic activity in the process of deep oxidation of CO and propane. It should be noted that flasks are similar in composition and structure to diatomite, so it can be expected that diatomite-based composites will also exhibit high catalytic activity.

The results of the elemental analysis of the surface of composite granules according to SEM/EDS data at points in Figs. 6 and 7 are presented in Tables 1 and 2.

According to Table 2, significant levels of impurity elements (Na, K, Mg, Ca, Al, and Fe) are observed in both the carrier and finished composite samples. This is related to the natural origin of diatomite and depends on the specific deposit. The highest concentrations are indicated for iron-containing phases, which impart a characteristic reddish-brown hue to the original diatomite samples.

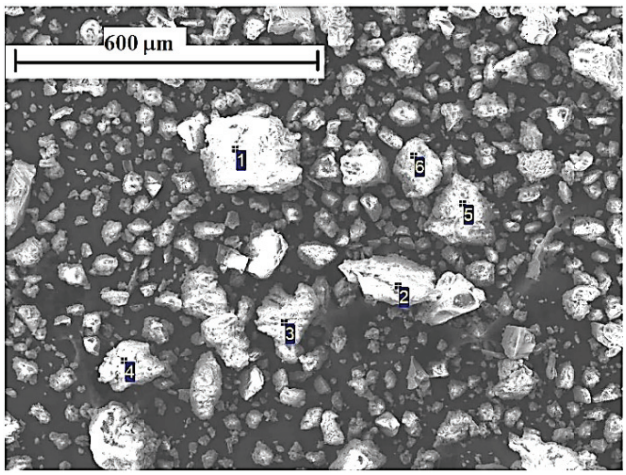

Fig. 6. SEM-image of D2 sample

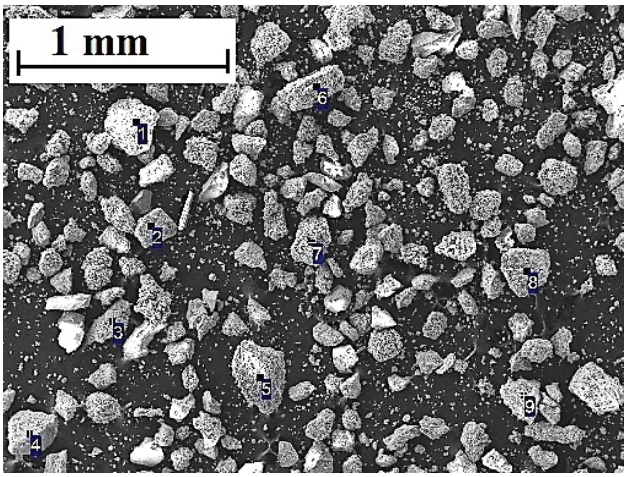

Fig. 7. SEM-image of catalyst sample 5Co5Mn/D2

Table 1. Elemental composition of the surface (wt. %) of the D2 sample in the points in Fig. 6

Point number	Elements, wt. %						
	O	Mg	Al	Si	K	Ca	Fe
1	31.91	0.52	1.50	41.16	2.36	1.32	21.23
2	35.75	0.42	1.88	21.96	0.95	0.56	38.48
3	58.40	0.58	4.64	32.79	1.32	0.42	1.85
4	49.14	0.56	4.57	40.25	1.63	0.73	3.12
5	67.28	0.13	1.87	29.62	0.42	0.23	0.45
6	63.19	0.44	2.66	32.08	0.62	0.30	0.67
Mean	51.08	0.44	2.85	33.05	1.22	0.60	10.76

Table 2. Elemental composition of the surface (wt. %) of the 5Co5Mn/D2 sample in the points in Fig. 7

Point number	Elements, wt. %										
	O	Na	Mg	Al	Si	K	Ca	Ti	Mn	Fe	Co
1	57.25	0.60	0.43	3.44	28.05	0.54	0.55	0.77	3.78	1.04	3.55
2	24.47	0.00	0.10	2.65	13.07	1.12	0.85	0.44	25.55	1.37	27.39
3	56.16	0.13	0.31	2.02	29.33	0.33	0.55	0.15	5.05	0.97	5.00
4	11.82	0.00	0.18	1.45	10.84	1.48	1.58	0.95	32.25	6.52	32.93
5	54.50	0.20	0.31	1.95	23.76	0.52	0.65	0	8.28	1.74	8.12
6	33.74	0.08	0.26	3.32	34.75	0.97	0.80	0.05	11.53	2.24	12.25
7	18.87	0.00	0.08	2.09	11.24	0.10	0.64	0.00	29.16	6.73	31.09
8	29.46	0.30	0.65	3.03	28.79	0.62	2.04	0.82	14.89	7.51	12.26
9	5.07	0.00	0.11	2.77	4.95	0.60	2.19	0.00	31.52	12.86	39.94
Mean	32.37	0.15	0.23	2.55	20.47	0.69	1.09	0.35	18.13	4.92	19.17

Note the wide range of concentrations of cobalt- and manganese-containing phases on the surface of various composite granules, apparently related to the varying absorption of the initial precursor solution by the individual granules. This absorption, in turn, depends on the wettability and pore structure of the individual granules, which varies greatly due to the structural heterogeneity of natural minerals. This heterogeneity manifests itself when the carrier is crushed into granules of different types. Even visually, Figs. 6 and 7 reveal granules with a denser surface and granules that are essentially conglomerates of small particles. However, the higher average Co and Mn contents, compared to the calculated values, indicate that the metal-containing phases are concentrated primarily on the outer surface of the granules. The surface morphology of the composite granules is shown in more detail in Fig. 8.

To study the surface morphology of the composite in Fig. 8, composite granules based on two main types of carrier granules were selected. Granules of the first type (Fig. 8*a*) are denser, layered, and covered with micron-sized crystallites. However, at the nanoscale, a flaky surface structure appears, with characteristic flake sizes < 200 nm. The composition of these morphological elements, due to their size, cannot be analyzed by EDS. Since the specific surface area of this composite sample is smaller than that of its carrier (see Fig. 5), the morphology of the metal-containing phase can be associated with the noted micron-sized crystallites on the surface. Granules of the second type (Fig. 8*b*) have the appearance of loose breccia-type conglomerates; however, at the nanoscale, in contrast to granules of the first type, their stepped surface is smoother and permeated with nanopores. No details that could be associated with the deposited phase are observed at this level.

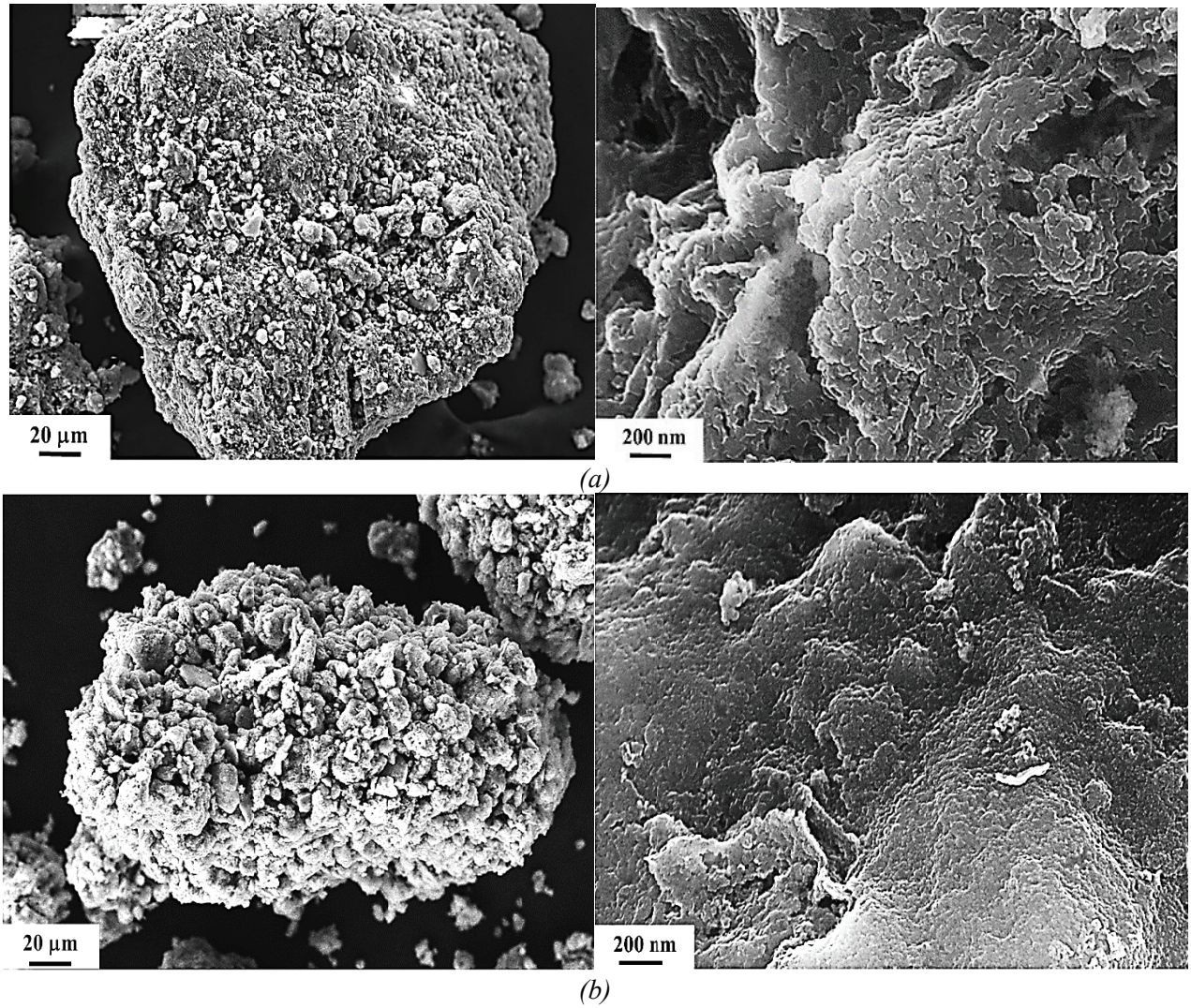

Fig. 8. SEM-images of two 5Co5Mn/D2 composite granules of different structure

4. Conclusion

Composite materials with a deposited Co-Mn-containing phase were obtained using low-temperature combustion on the basis of natural and activated diatomite samples. These materials were then used as catalysts in the deep oxidation of CO and hydrocarbons. In addition to the original diatomite (D1), three types of activated diatomites were obtained: those calcined at 500 °C (D2), those treated with an HCl solution (D3), and those treated with an HCl solution and then calcined at 500 °C (D4). Synthesis of the composites by low-temperature combustion included the following steps: impregnation of the diatomite samples with solutions of Co and Mn nitrates (oxidizers) and urea (reducing agent, fuel), drying, and initiation of the combustion process by heating the impregnated samples. The process was visually observed in the combustion wave mode. The maximum temperature in the combustion wave (337 °C) was recorded during the synthesis of the 5Co5Mn/D1 composite. In the thermograms of the synthesis of three composite samples, in addition to 5Co5Mn/D1, secondary peaks were observed, apparently associated with the passage of afterburning waves due to a complex, possibly autocatalytic combustion mechanism. According to XRD data, only peaks of various SiO_2 phases (quartz, tridymite, and cristobalite) were observed in the composites. The specific surface area of the composites ranged from 46.4 to 78.5 $m^2 \cdot g^{-1}$. EDS analysis revealed a significant spread in the surface concentrations of Co and Mn, mainly on two types of granules, apparently associated with the structural heterogeneity of natural diatomite. Noticeable concentrations of impurity elements, including iron, were also detected. The SEM morphology of composite granules with two different surface types was studied. Some assumptions are

made about the morphology of the Co-Mn-containing phases. The resulting composites are similar in composition to our previously synthesized 5Co5Mn/opoka composites, which demonstrated high catalytic activity in the deep oxidation of CO and propane. Since these diatomite-based composites have a significantly higher specific surface area (approximately 15 $m^2 \cdot g^{-1}$) compared to 5Co5Mn/opoka, their high catalytic activity can be assumed.

5. Funding

The study was conducted on the ISMAN state assignment.

R.I. Jussupkaliyeva is grateful to the Ministry of Science and Higher Education of the Republic of Kazakhstan for the financial support.

6. Conflict of interest

The authors declare no conflict of interest.

References

1. Smirnov PV, Konstantinov AO, Gursky HJ. Petrology and industrial application of main diatomite deposits in the Transuralian region (Russian Federation). *Environmental Earth Sciences*. 2017;76(20):682. DOI:10.1007/s12665-017-7037-3

2. YergozhinEE, Akimbayeva AM. *Organomineral sorbents and polyfunctional systems based on natural aluminosilicate and coal-mineral raw materials.* Almaty: TOO "Print-S" Publ. House; 2007. 373 p. (In Russ.)

3. Makarova I, Faizov R, Buzaeva M, Davydova O, et al. Utilization of nanomodified dispersion of lubricating coolants with the use of natural sorbents. *Bulletin of the South Ural State University series "Chemistry"*. 2017;9(2):5-12. DOI:10.14529/chem170201

4. Aivalioti M, Papoulias P, Kousaiti A, Gidarakos E. Adsorption of BTEX, MTBE and TAME on natural and modified diatomite. *Journal of Hazardous Materials*. 2012;207-208:117-127. DOI:10.1016/j.jhazmat.2011.03.040

5. Xie F, Wu F, Liu G, Mu Y, et al. Removal of phosphate from eutrophic lakes through adsorption by in situ formation of magnesium hydroxide from diatomite. *Environmental Science & Technology*. 2014;48(1):582-590. DOI:10.1021/es4037379

6. Ma T, Wu Y, Liu N, Wu Y. Hydrolyzed polyacrylamide modified diatomite waste as a novel adsorbent for organic dye removal: adsorption performance and mechanism studies. *Polyhedron*. 2020;175:114227. DOI:10.1016/j.poly.2019.114227

7. Tao X, Wu Y, Sha H. Cuprous oxide-modified diatomite waste from the brewery used as an effective adsorbent for removal of organic dye: adsorption performance, kinetics and mechanism studies. *Water, Air, & Soil Pollution*. 2018;229(10):322. DOI:10.1007/s11270-018-3977-9

8. Rudakov VM, Agladze MG, Kolpakova EE, Kazakov JuM, Davydova GI. Polymerization of ethylene on the surface of diatomites and other natural silica rocks activated by an organoaluminum compound. *Vysokomolekulyarnye soedineniya. Seriya B.* 1992;34(5): 37-43. (In Russ.)

9. Nazhipkyzy M, Nemkayeva RR, Nurgain A, Seitkazinova AR, et al. The use of diatomite as a catalyst carrier for the synthesis of carbon nanotubes. *Nanomaterials*. 2022;12(11):1817. DOI:10.3390/nano12111817

10. Agabekov VE, Sen'kov GM, Sidorenko AYu, Tuyen ND, et al. New α-pinene isomerization catalysts. *Catalysis in Industry*. 2011;3(4):319-330. DOI:10.1134/S2070050411040027

11. Toshtay K, Auezov AB. Hydrogenation of vegetable oils over a palladium catalyst supported on activated diatomite. *Catalysis in Industry*. 2020;12(1):7-15. DOI:10.1134/S2070050420010109

12. Liang L, Miao C, Ke X, Peng Y, et al. A superior strategy for CO_2 methanation under atmospheric pressure: organic acid-assisted co nanoparticles assembly on diatomite. *Fuel*. 2023;351:128931. DOI:10.1016/j.fuel.2023.128931

13. Liu Q, Li M, Wang S, Lv S, et al. Ultrathin 3D CoMn nanoflowers coupled diatomite for highly efficient catalytic oxidation of CO and propane. *Chemical Engineering Journal*. 2023;477:147102. DOI:10.1016/j.cej.2023.147102

14. Zhang X, Shen J, Sun H, Gong Y, et al. Room temperature oxidation of formaldehyde using TiO_2/recycled diatomite composite. *Journal of the Minerals, Metals & Materials Society*. 2022;74(7):2716-2723. DOI:10.1007/s11837-022-05224-0

15. Han Z, Wang C, Zou X, Chen T, et al. Diatomite-supported birnessite-type MnO_2 catalytic oxidation of formaldehyde: preparation, performance and mechanism. *Applied Surface Science*. 2020;502:144201. DOI:10.1016/j.apsusc.2019.144201

16. Yang Y, Zhang Z, Li Y, Wang R, et al. The catalytic aerial oxidation of As(III) in alkaline solution by Mn-loaded diatomite. *Journal of Environmental Management*. 2022;317:115380. DOI:10.1016/j.jenvman.2022.115380

17. Matskan PA, Evdokimova EV, Mamontov GV. MIL-100(Fe)/diatomite composites for photo-fenton

degradation of phenol. *Kinetika ikataliz = Kinetics and Catalysis*. 2023;64(4):418-427. DOI:10.31857/S045388112304007X (In Russ.)

18. Dai N, Yi S, Zhang X, Feng L, et al. Typical synthesis of an iron-modified laponite @diatomite composite for photo-fenton degradation of methyl orange dyes. *Applied Surface Science*. 2023;607:154886. DOI:10.1016/j.apsusc.2022.154886

19. Ge Y, Xu HQ, Huang Q, Jia X, et al. Microwave-assisted synthesis of Ag/ZnO/diatomite composites for photocatalytic degradation of gaseous toluene. *Inorganic Chemistry Communications*. 2025;171:113543. DOI:10.1016/j.inoche.2024.113543

20. Rezig W, Elaziouti A, Laouedj N, Hadjel M. Synthesis and characterization of novel calcined ferrihydrite-modified diatomite (FMD3X6) and its UVA light-assisted heterogeneous photodegradation of VG3 dye. *Desalination and Water Treatment*. 2022;271:254-271. DOI:10.5004/dwt.2022.28719

21. Datsko TY, Zelentsov VI. Hybrid nano-titanium dioxide/diatomite photocatalyst for advanced oxidation processes (AOPs) mediated removal of toxic organic pollutants. *Chemical Safety Science.* 2020;4(2):101-116. DOI:10.25514/CHS.2020.2.18007

22. Xu H, Wang H, Wang X, Tang Z, et al. Fluidized bed photobioreactor based on diatomite powder and high light intensity improved microalgae harvesting, nutrient removal and lipid accumulation: Performance and microscopic mechanism. *Water Research*. 2024;264:122172. DOI:10.1016/j.watres.2024.122172

23. Borshch VN, Zhuk SYa, Vakin NA, Smirnov KL, et al. Sialons as a new class of supports for oxidation catalysts. *Doklady Physical Chemistry*. 2008;420(2):121-124. DOI:10.1134/S0012501608060018

24. Zav'yalova UF, Tret'yakov VF, Burdeinaya TN, Lunin VV, et al. Self-propagating synthesis of supported oxide catalysts for deep oxidation of CO and hydrocarbons. *Kinetics and Catalysis*. 2005:46(5):752-757. DOI:10.1007/s10975-005-0132-6

25. Zavyalova U, Scholz P, Ondruschka B. Influence of cobalt precursor and fuels on the performance of combustion synthesized Co_3O_4/γ-Al_2O_3 catalysts for total oxidation of methane. *Applied Catalysis A: General*. 2007:323:226-233. DOI:10.1016/j.apcata.2007.02.021

26. Kotolevich YS, Khramov EV, Mironenko OO, Zubavichus YaV, et al. Supported palladium catalysts prepared by surface self-propagating thermal synthesis. *International Journal of Self-Propagating High-Temperature Synthesis*. 2014;23(1):9-17. DOI:10.3103/S1061386214010075

27. Smagulova GT, Prikhod'ko NG, Guseinov NR, Nemkayeva R, et al. Zeolite based catalysts for synthesis of carbon nanotubes. *Goreniye i plazmoximia*. 2016;14(2):83-88. (In Russ.)

28. Kotolevich YS, Mamontov GV, Vodyankina OV, et al. Catalytic Pd-Ag nanoparticles immobilized on fiber glass by surface self-propagating thermal synthesis. *International Journal of Self-Propagating High-Temperature Synthesis*. 2017;26:234-239. DOI:10.3103/S1061386217040045

29. Borshch VN, Dement'eva IM, Khomenko NYu. Supported polymetallic catalysts by self-propagating surface synthesis. *International Journal of Self-Propagating High-Temperature Synthesis*. 2019;28(1):45-49. DOI:10.3103/S1061386219010059

30. Borshch VN, Bystrova IM, Pugacheva EV, Smirnova EM, et al. Low-temperature combustion synthesis of halloysite-based catalysts for the deep oxidation of hydrocarbons and carbon monoxide and the methanation of carbon dioxide. *Kinetics and Catalysis*. 2022;63(6):801-812. DOI:10.1134/S0023158422060027

31. Borshch VN, Bystrova IM, Pugacheva EV, Khomenko NYu. Hydrogenation of CO_2 on Co-Ni catalysts produced by low-temperature combustion using modified silica fabric. *International Journal of Self-Propagating High-Temperature Synthesis*. 2023;32(4):302-312. DOI:10.3103/S1061386223040131

32. Borshch VN, Bystrova IM, Boyarchenko OD, Khomenko NYu, et al. Low-temperature combustion synthesis and characterization of Co-containing catalysts based on modified silica gel. *International Journal of Self-Propagating High-Temperature Synthesis*. 2023;32(2):126-138. DOI:10.3103/S1061386223020024

33. Li G, Li N, Sun Y, Qu Y, et al. Efficient defect engineering in Co-Mn binary oxides for low-temperature propane oxidation. *Applied Catalysis B: Environmental*. 2021;282:119512. DOI:10.1016/j.apcatb.2020.119512

34. Shan C, Zhang Y, Zhao Q, Li J, et al. New insight into opposite oxidation behavior in acetone and propane catalytic oxidation over CoMn based spinel oxides. *Chemical Engineering Journal*. 2023;476:146550. DOI:10.1016/j.cej.2023.146550

35. Zhao H, Wang H, Qu Z. Synergistic effects in Mn-Co mixed oxide supported on cordierite honeycomb for catalytic deep oxidation of VOCs. *Journal of Environmental Sciences*. 2022;112:231-243. DOI:10.1016/j.jes.2021.05.003

36. Jussupkaliyeva RI, Bystrova IM, Pomogailo SI, Borshch VN. Synthesis of Co-Mn catalysts for deep oxidation of CO and propane based on natural opoka by low-temperature combustion. *Izvestiya vysshikh uchebnykh zavedeniy. Poroshkovaya metallurgiya i funktsional'nye pokrytiya = Powder Metallurgy and Functional Coatings.* 2024;18(6):17-27. DOI:10.17073/1997-308X-2024-6-17-27 (In Russ.)

Information about the authors / Информация об авторах

Roza I. Jussupkaliyeva, Senior Lecturer, Zhangir Khan West Kazakhstan Agrarian Technical University, Uralsk, Republic of Kazakhstan; ORCID 0000-0001-8916-0008; e-mail: Rozaid2@mail.ru

Vyacheslav N. Borshch, Cand. Sc (Chem.), Leading Researcher, Merzhanov Institute of Structural Macrokinetics and Materials Science RAS (ISMAN), Chernogolovka, Russian Federation; ORCID 0000-0001-5827-4942; e-mail: borsch @ism.ac.ru

Inna M. Bystrova, Junior Research Fellow, ISMAN, Chernogolovka, Russian Federation; ORCID 0000-0003-3739-7390; e-mail: inna2019@ism.ac.ru

Elena V. Pugacheva, Cand. Sc (Chem.), Senior Researcher, ISMAN, Chernogolovka, Russian Federation; ORCID 0000-0002-4354-8776; e-mail: help@ism.ac.ru

Natalia Yu. Khomenko, Senior Researcher, ISMAN, Chernogolovka, Russian Federation; ORCID 0000-0001-9388-7365; e-mail: khomenko@ism.ac.ru

Artem V. Rukhov, D. Sc. (Eng.), Professor, Head of the Department, Tambov State Technical University, Tambov, Russian Federation; ORCID 0000-0001-9194-8099; e-mail: rukhov.av@gmail.com

Svetlana I. Pomogailo, Cand. Sc. (Chem.), Senior Researcher, ISMAN, Chernogolovka, Russian Federation; Senior Researcher, All-Russian Institute for Scientific and Technical Information, Moscow, Russian Federation ORCID 0000-0001-8200-0706; e-mail: pom_lana@ism.ac.ru

Джусупкалиева Роза Ибраимовна, старший преподаватель, Западно-Казахстанский аграрно-технический университет имени Жангир хана, Уральск, Республика Казахстан; ORCID 0000-0001-8916-0008; e-mail: Rozaid2@mail.ru

Борщ Вячеслав Николаевич, кандидат химических наук, ведущий научный сотрудник, Институт структурной макрокинетики и проблем материаловедения им. А. Г. Мержанова РАН (ИСМАН), Черноголовка, Российская Федерация; ORCID 0000-0001-5827-4942; e-mail: borsch @ism.ac.ru

Быстрова Инна Михайловна, младший научный сотрудник, ИСМАН, Черноголовка, Российская Федерация; ORCID 0000-0003-3739-7390; e-mail: inna2019@ism.ac.ru

Пугачева Елена Викторовна, кандидат химических наук, старший научный сотрудник, ИСМАН, Черноголовка, Российская Федерация; ORCID 0000-0002-4354-8776; e-mail: help@ism.ac.ru

Хоменко Наталья Юрьевна, старший научный сотрудник, ИСМАН, Черноголовка, Российская Федерация; ORCID 0000-0001-9388-7365; e-mail: khomenko@ism.ac.ru

Рухов Артём Викторович, доктор технических наук, профессор, заведующий кафедрой, Тамбовский государственный технический университет, Тамбов, Российская Федерация; ORCID 0000-0001-9194-8099; e-mail: rukhov.av@gmail.com

Помогайло Светлана Ибрагимовна, кандидат химических наук, старший научный сотрудник, ИСМАН, Черноголовка, Российская Федерация; старший научный сотрудник, Всероссийский институт научной и технической информации РАН, Москва, Российская Федерация ORCID 0000-0001-8200-0706; e-mail: pom_lana@ism.ac.ru

Received 30 May 2025; Revised 25 July 2025; Accepted 07 August 2025